AAPS PharmSciTech (2024) 25:31
https://doi.org/10.1208/s12249-024-02750-9

RESEARCH ARTICLE

Advancements in Amorphous Solid Dispersions to Improve Bioavailability

Spray-Dried Mucoadhesive Re-dispersible Gargle of Chlorhexidine for Improved Response Against Throat Infection: Formulation Development, *In Vitro* and *In Vivo* Evaluation

Vineet Kumar Rai[1] · Amresh Kumar[2] · Deepak Pradhan[1] · Jitu Halder[1] · Tushar Kanti Rajwar[1] · Manoj Kumar Sarangi[3] · Priyanka Dash[1] · Chandan Das[1] · Salim Manoharadas[4] · Biswakanth Kar[1] · Goutam Ghosh[1] · Goutam Rath[1]

Received: 25 October 2023 / Accepted: 20 January 2024 / Published online: 7 February 2024

Abstract

Drug delivery to the buccal mucosa is one of the most convenient ways to treat common mouth problems. Here, we propose a spray-dried re-dispersible mucoadhesive controlled release gargle formulation to improve the efficacy of chlorhexidine. The present investigation portrays an approach to get stable and free-flowing spray-dried porous aggregates of chlorhexidine-loaded sodium alginate nanoparticles. The ionic gelation technique aided with the chlorhexidine's positive surface charge–based crosslinking, followed by spray drying of the nanoparticle's dispersion in the presence of lactose- and leucine-yielded nano-aggregates with good flow properties and with a size range of about 120–350 nm. Provided with the high entrapment efficiency (87%), the particles showed sustained drug release behaviors over a duration of 10 h, where 87% of the released drug got permeated within 12 h. The antimicrobial activity of the prepared formulation was tested on *S. aureus*, provided with a higher zone of growth inhibition than the marketed formulation. Aided with an appropriate mucoadhesive strength, this product exhibited extended retention of nanoparticles in the throat region, as shown by *in vivo* imaging results. In conclusion, the technology, provided with high drug retention and extended effect, could be a potential candidate for treating several types of throat infections.

Keywords chlorhexidine · gargle · mucoadhesive · re-dispersible · spray drying · sodium alginate · throat infection

Introduction

The advent of various novel drug delivery approaches indicates several disadvantages associated with conventional drug delivery systems such as the need for higher doses due to hepatic first-pass metabolism and systemic toxicity resulting from the higher drug dose [1]. There is a lot of interest in drug administration through the buccal mucosa since it offers the benefit of direct drug availability locally or into the systemic circulation through the reticulated vein lining of the buccal mucosa, thereby avoiding hepatic first-pass metabolism [1–4]. Mucosal sites are considered attractive for local drug administration due to their unique benefits, which include low enzymatic activity, high blood flow, easy accessibility, high sialic acid, and required surface area [1]. Mucoadhesive formulations are meant to adhere to the buccal wall through an interaction with the mucus, thus favoring longer residence time [5]. First-generation mucoadhesive polymers bind to mucin through non-covalent interactions, while the next generation, including thiolated polymers, adheres to mucin through covalent bonds [6]. However, hydrophilicity, molecular weight, concentration, swelling factor, degree of crosslinking of polymers, as well

✉ Goutam Rath
goutamrath123@gmail.com

1 Department of Pharmacognosy, School of Pharmaceutical Sciences, Siksha 'O' Anusandhan (Deemed to Be University), Bhubaneswar, Odisha 751003, India

2 Department of Pharmaceutics, I.S.F. College of Pharmacy, Moga, Punjab, India

3 Department of Pharmaceutics, Amity Institute of Pharmacy, Amity University, Lucknow, Uttar Pradesh, India

4 Department of Botany and Microbiology, College of Science, King Saud University, P.O. Box. 2454, 11451 Riyadh, Saudi Arabia

as physiological conditions like the presence of a disease, mucin turnover rate, and local pH, must all be taken into account to ensure the optimum performance of mucoadhesive drug delivery systems [7].

Polymeric nanoparticles are suitable drug carriers for buccal drug delivery because of their unique ability to provide controlled release of encapsulated bioactive at the target site, accumulation at the target site, and protection from degradation from the external biological environment. Due to the advantages of improving drug localization and encouraging the need for smaller therapeutic doses, polymeric nanoparticles seem to be the preferred drug delivery carrier for buccal use. Additionally, polymeric nanoparticles with a high surface-to-volume ratio have more vital attractive forces with mucus, resulting in longer retention at the application site [4, 8]. The surface charge of nanoparticles that binds to the negatively charged mucin contributes to their mucoadhesive nature [4, 5]. Mucoadhesive nanoparticles for buccal administration are fabricated from various polymers such as chitosan, alginate, poly(acrylic acid), cellulose derivatives, polyvinyl alcohol, and polyethene glycol [8].

Sodium alginate is a hydrophilic natural polymer which is biocompatible, biodegradable, and included in GRAS categories by FDA. Chemically, it is a polysaccharide, a monovalent form of alginic acid having β-D-mannuronic acid and α-L-guluronic acid as two monomeric units [9]. Due to the presence of carboxylic ends, sodium alginate is categorized as an anionic mucoadhesive polymer which is considered to have greater extent of bio-adhesion as compared to polycationic mucoadhesive polymers [10]. Sodium alginate undergoes rapid gelation in the presence of divalent or polyvalent cations, forming an insoluble network [11]. This is formed due to the polymer's ionic interaction and intermolecular bonding between cations and carboxylic acid groups [9]. Sodium alginate may often be blended with other suitable mucoadhesive polymers to enhance the functional properties of a formulation, such as swelling, stability, drug encapsulation, and release [12].

Chlorhexidine is a biguanide wide-spectrum topical antimicrobial agent used as a significant component of daily mouthwash to treat gingivitis. Chlorhexidine can be used to treat several severe disorders, including endodontics and infected oral mucositis. In contrast to antibiotics, it is a biocide and is less likely to acquire resistance [13, 14]. It targets the membrane integrity of microorganisms at low concentrations, while coagulation of the cytoplasm occurs at higher concentrations. Chlorhexidine is a pH-sensitive antimicrobial agent, with pH 7.0 being optimal [14]. Incorporation or encapsulation of chlorhexidine into nanocarriers can improve overall biological activity due to enhanced retention at the target site [15]. This further helps to lower the possibility of the emergence of drug resistance [14].

In the present study, chlorhexidine-loaded sodium alginate nanoparticles were fabricated to treat throat infections. The ionic gelation method was utilized to prepare the nanoparticles with chlorhexidine as the crosslinker, which was also the active constituent. The prepared nanoparticles were further spray-dried in the presence of L-lucine and lactose to increase the yield and flow properties of the nanoparticles. Finally, the modified nanoparticles were subjected to various *in vitro* and *in vivo* evaluation parameters to justify their hypothesized application.

Materials

Chlorhexidine was obtained from Cadila Pharmaceutical Limited, New Delhi. Acetonitrile HPLC grade was purchased from SD Fine-Chemie Pvt, Ltd., Mumbai. Barium sulfate was purchased from Loba Chemie Pvt., Ltd., Mumbai, India. Chlorhexidine was purchased from Zydus Cadila Pharmaceutical, New Delhi, and DMSO, ethanol, orthophosphoric acid, potassium hydroxide, sodium alginate, sodium chloride, hydrochloric acid, L-luciene, and Tween 20 was purchased from Central Drug House, New Delhi. Lactose, dialysis membrane, n-octanol, methanol, potassium chloride, potassium hydrogen phosphate, and sodium hydrogen phosphate were purchased from HiMedia Laboratories Pvt. Ltd., Mumbai. All other chemicals used were of analytical grade.

Methods

Determination of λ_{max} and Preparation of Standard Curve

The λ_{max} of the drug was confirmed by making stock solutions of known concentrations 100 µg/mL of chlorhexidine gluconate in water. This was then scanned by UV-spectrophotometer (Schimadzu Corporation, Japan) in the range of 400 to 200 nm, and absorption maxima was determined. Furthermore, several dilutions of the drug were prepared in increasing order (2, 4, 6, 8, 10, 12, and 14 µg/mL), and the absorbance was measured at the λ_{max} of 253 nm. Finally, a graph between drug concentration and absorbances was plotted, and the linearity of the curve was determined [16].

Preparation and Optimization of Nanoparticle

In the present study, chlorhexidine gluconate–loaded sodium alginate nanoparticle was prepared by using the ionic gelation method. The positive charge of chlorhexidine interacted with the negative charge of sodium alginate to

form coacervates with a size in the range of nanometers. Chlorhexidine gluconate was used in the 0.3 to 1.2% range to optimize crosslinking. Sodium alginate was used in the range of 0.1 to 0.4%. The sodium alginate was added to the solution of chlorhexidine gluconate drop by drop using a dropper under continuous high-speed (6000 rpm) stirring at a fixed concentration of tween 20 [17].

Preparation of Spray-Dried Powder

Labultima spray dryer was used to prepare re-dispersible spray-dried nanoaggregates. Each stock solution of chlorhexidine gluconate–loaded sodium alginate nanoparticle was mixed with a bulking agent (lactose) and anti-adherent (leucine) at 5% w/v. The inlet temperature was maintained at 90–95°C, outlet temperature at 70–75°C and vacuum at 78–95 Pa. Incorporation of leucine into the formulation before spray-drying could improve process yield because of its anti-adherent and hydrophobic properties [18, 19].

Characterization of the Developed Spray-Dried Powder

Particle Size and Size Distribution

The optimized nanoparticles' particle size and size distribution and nanospray-dried powdered particle were determined by laser diffractometer-based Beckman coulter Delsa TM Nano C Particle analyzer. The cuvettes were cleaned with distilled water to reduce the possibility of contamination. For the measurement of size and polydispersity index (PDI), 2-mL particular dispersions were placed into cuvette of Beckman coulter, and measurements were recorded.

Drug Polymer Interaction or Compatibility Studies

FTIR study was performed for identifying and analyzing possible interaction in the tested samples. An IR spectrum of the pure drug and spray-dried powders were obtained by crushing them with potassium bromide (KBr) in mortar and pestle into fine powder and making their pellets by maintaining the pressure of 10 tons for a minute. Infrared spectrum was recorded by scanning over a wave number region of 400–4000 cm^{-1} using Nicolet software.

Micrometric Properties of the Powder

Spray-dried powder was characterized for its flow properties utilizing variables such as the angle of repose, bulk density, tapped density, Hausner's ratio, Carr's, and compressibility index. The results were expressed as mean values of three determinations. As far as angle of repose is concerned, the powdered sample is allowed to fall gently through a funnel on to a hard surface from the height of 2.5 cm. The height of the pile and diameter were noted. Angle of repose was determined by using the formula Angle of repose $(\theta) = tan^{-1}(h/r)$. Where, h is the height and r are the radius of the powder cone. For bulk density determination, 10-g powder sample was weighed and was gently poured through glass funnel into calibrated 100-mL measuring cylinder. The volume occupied by the sample was recorded, and bulk density (g/mL) was calculated and recorded in the table by using formula $\text{Bulk density} = \frac{\text{Weight of sample taken}}{\text{Bulk volume}}$. Similarly, as bulk density, tapped density was observed by tapping the cylinder 100 times from 2-inch height by using Electrotab-tapped density apparatus after pouring the pellets into the measuring cylinder and the tapped volume was recorded. Finally, the tapped density was recorded by using the formula $\text{Tapped density} = \frac{\text{Weight of sample taken}}{\text{Tapped volume}}$. The Hausner's ratio is a number that is correlated to the flowability of powder. It was calculated as the ratio of tapped density and bulk density. However, Carr's index is an indication of the compressibility of pellets. Formula $\text{Carr}'\text{sindex}(\%) = \frac{\rho t - \rho b}{\rho t} \times 100$ is used to determine Carr's index in which Pt is tapped density and ρb is bulk density [20, 21].

Scanning Electron Microscopy

Scanning electron microscopy (SEM; ZEISS, Evo 18, Thornwood, NY, USA) was employed to analyze the prepared nanoparticle's shape and size. A gold sputter–coated particle mat was kept in the SEM sample holder. The SEM images were taken using an accelerating voltage of 20 kV. We examined up to 10 different locations on a particle mat to assess the average diameter of the NPs. Three viewing fields were selected at different magnifications for resolution.

Crystalline Structure Assessment

Powder X-ray diffraction (XRD) is one of the most precise methods for characterizing the phase behavior of the drug in nanoparticles. It was done as per the procedure reported elsewhere by Shrimal *et al.* [22]. The prepared powdered samples were investigated for crystallinity using a monochromic Cu-Kα radiation wavelength ($\lambda = 1.5418$ Å) BRUKER D8 Advance Diffractometer.

Determination of Entrapment Efficiency

Chlorhexidine gluconate–loaded nanoparticles and spray-dried powdered dispersions were centrifuged at 12,000 rpm for 1 h. Then, 1 mL of supernatant was taken and diluted up

to 100 mL with water. Finally, drug content was analyzed at 253 nm using a UV-spectrophotometer. EE was calculated using the following formula:

$$\% \text{ EE} = \frac{\text{Total amount of drug added} - \text{Amount of untrapped drug}}{\text{Total amount of drug added}} \times 100$$

In Vitro Drug Release Study

Release of chlorhexidine gluconate from spray-dried powder, marketed formulation and plain drug was evaluated *in vitro* using the dialysis bag method in phosphate buffer 7.4. Before the commencement of the experiment, the dialysis bag (molecular weight cutoff 8–14 kDa; Sigma Aldrich) was washed thoroughly with deionized water to remove the preservatives. Samples equivalent to 10 mg of chlorhexidine gluconate were dispersed in distilled water and transferred to a dialysis bag. The bags were tied with threads at both ends and immersed in a beaker with 100-mL buffer. The system was shaken at 100 rpm on a magnetic stirrer at 37°C. The 2-mL aliquots were withdrawn at predetermined intervals of 15 min, 30 min, 45 min, 60 min, 120 min, 240 min, 360 min, 480 min, and 600 min, and the sample was analyzed at 253 nm by UV–VIS spectrophotometer after passing it through syringe filter of 0.22-µm pore size and diluting them with water to a suitable concentration to match the linearity range of the calibration curve. Further, 2 mL of fresh phosphate buffer was replaced immediately in each sample [23]. The study was done in triplicate, and the analyzed drug concentration was plotted against time to assess the dissolution rate of the drug from the developed formulation.

Ex Vivo Permeation Study

Permeation of chlorhexidine gluconate from the spray-dried powder, marketed formulation, and plain drug was evaluated by an *ex vivo* method using intestinal mucosal membrane. The samples equivalent to 10 mg of the pure drug was dispersed in 10-mL PBS and transferred inside the harvested intestine. The sampled intestinal portion was tied at both ends and immersed in a beaker containing 100-mL PBS. The system was shaken at 100 rpm on a magnetic stirrer at 37°C. Then, 2-mL aliquots were withdrawn at predetermined intervals of 15 min, 30 min, 45 min, 60 min, 120 min, 240 min, 360 min, 480 min, 600 min, and 720 min). Further, 2-mL fresh mixed in the medium to adjust the withdrawn volume of the sample. The collected samples were analyzed at 253 nm by UV–VIS spectrophotometer. The study was done in triplicate form [24, 25].

Mucoadhesive Strength

The mucoadhesive strength of the developed powder was tested using Brookfield's texture analyzer. The gout mucosa was placed on one of the attachments of the device and spray-dried powder stuck to the other attachment of the analyzer with the help of double-sided tape. The force needed for the spray dryer powder to detach from the mucosa was calculated [24].

In Vitro Antimicrobial Activity

The antimicrobial activity of prepared formulation was determined against *S. aureus* in Muller-Hinton broth. The nutrient broth was inoculated by using a swab dipped in the bacterial cell suspension. Sample (plain drug, marketed formulation, and drug-loaded formulation) were carefully placed on the agar surface for the evaluation and comparison of antimicrobial activity. The zones of inhibition were measured after 1 and 2 days [26].

In Vivo Investigation of Retention Time by X-ray

The retention efficacy of optimized formulation in rat was determined using a radiographic imaging technique. The animals were fasted overnight before the experiment, with free access to water. Formulation containing the contrast medium of 0.50% barium sulfate was administered orally with the help of pan-century insufflators. X-ray images of throat were taken at various time points up to 8 h to trace the *in vivo* movement and behavior of spray-dried nanoparticle. X-ray images of the rats were captured using L & T Vision 100 (C-arm) X-ray machine, at 64 mAs and 63-kV techniques [27].

Statistical Analysis

GraphPad Prism version 8 was used for the statistical analyses of the data. Means and standard deviations are used to express values at least in 3 replicates. One-way ANOVA test (post hoc test) and Student's *t* test were used to analyze and compare the variations. $P = 0.05$ was considered statistically significant.

Results and Discussion

Absorption Maxima and Calibration Curve of Chlorhexidine Gluconate

The wavelength at which maximum absorbance was observed was found to be 253 nm. The absorbance *vs*. wavelength curve is presented in Fig. 1a and b depicts the standard curve prepared on the measured absorption maxima. On this absorption maxima, the absorbances of various dilutions were noted and plotted against their respective

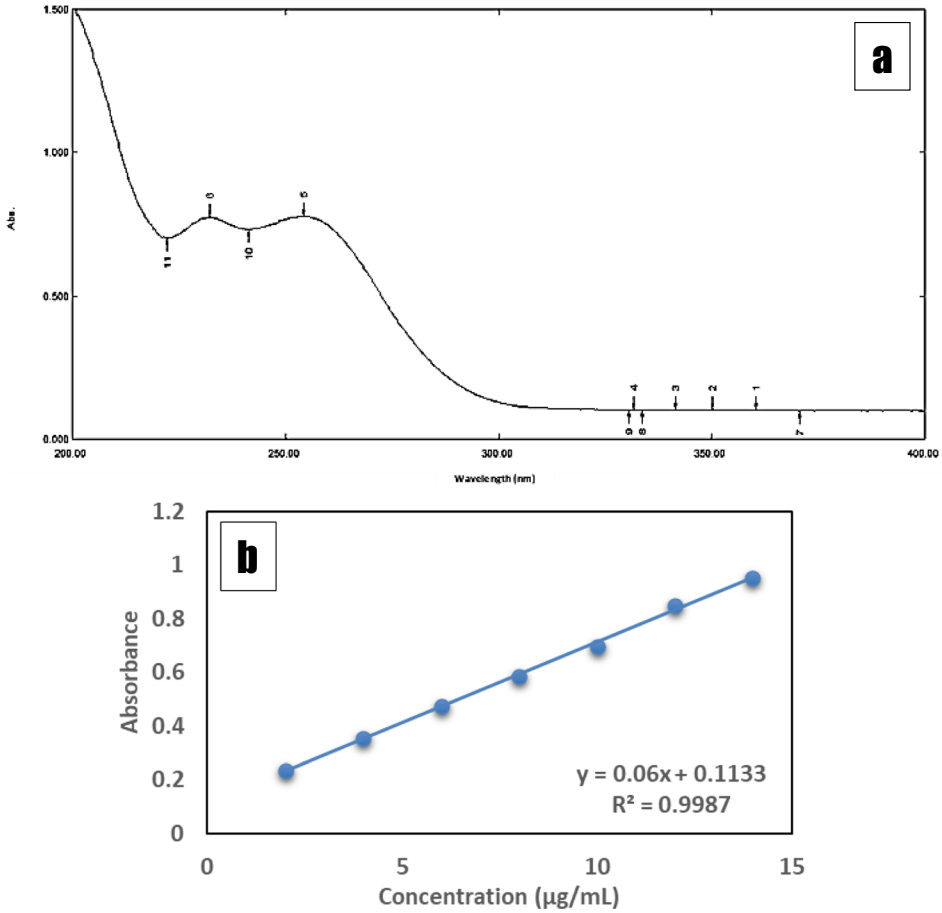

Fig. 1 Pictorial depiction of an UV-absorption spectra of chlorhexidine gluconate and its calibration curve. **a** UV-absorption spectra of chlorhexidine gluconate and **b** calibration curve of chlorhexidine gluconate

concentration. The linearity of the curve was found to be in the range of 2 to 14 µg/mL. The value for the regression coefficient was found to be 0.998 that portrayed a good correlation between the adjacent values.

Optimization of Nanoparticles

Table I shows the variation in particle size and PDI along with the change in experimental conditions like sodium alginate (%) and chlorhexidine gluconate (%). Change in chlorhexidine gluconate concentration from 0.3 to 1.2% and sodium alginate concentration from 0.1 to 0.4% had significant effect on particle size and PDI of the developed nanoparticles. At fixed sodium alginate concentration (0.1%), an increase in both particle size and PDI was obtained with change in chlorhexidine gluconate concentration from 0.3 to 1.2%. The pattern of increasing particle size and PDI with crosslinker's concentration may be due to random precipitation of alginate and formation of uneven structure. At higher crosslinker concentration, a higher degree of crosslinking is being observed due to which a higher particle aggregates could be observed. The polymers concentration seems not sufficient for producing compact structure with uniform distribution. At higher alginate concentration, i.e., 0.2%w/v, a significant decrease in particle size and PDI (from 440.5 ± 17.23 to 318.2 ± 16.78 and 0.364 ± 0.174 to 0.302 ± 0.074, respectively) was observed with the crosslinker's concentration from 0.3 to 0.5%v/v; however, a steep increase in particle size and PDI was observed at 0.6 and 0.8%v/v crosslinker. Since the particle size is being decreased with crosslinker concentration in the initial batches, it means particles with compact structure are being formed. However, after a limit, both particle size and PDI are being increased confirming 0.2%w/v with 0.5%v/v crosslinker concentration as the optimum combination with smallest particle size and uniform distribution of the particles. At 0.3%w/v sodium alginate, larger particle was observed at 0.3%v/v concentration of crosslinker. However, PDI was found to be increased from 0.3 to 0.5%v/v concentration of chlorhexidine gluconate. The same pattern was observed in the batches prepared at fixed concentration of sodium alginate (0.4%w/v) and with increasing concentration of crosslinker. A decrease in particle size and increase in PDI denotes the presence of two or more types of particles. The aforementioned

Table I Shows Optimization of Nanoparticles in Different Concentrations of Ingredients

Batches	Sodium alginate (% w/v)	Chlorhexidine gluconate (% v/v)	Tween 20 (%v/v)	Particle size (nm)	PDI
F1	0.10	0.30	0.1	328.8 ± 13.27	0.169 ± 0.120
F2	0.10	0.40	0.1	400.5 ± 23.62	0.200 ± 0.028
F3	0.10	0.50	0.1	528.4 ± 14.37	0.242 ± 0.016
F4	0.10	0.60	0.1	626.1 ± 17.35	0.413 ± 0.033
F5	0.10	0.80	0.1	876.6 ± 23.15	0.652 ± 0.089
F6	0.10	1.00	0.1	881.9 ± 19.58	0.828 ± 0.073
F7	0.10	1.20	0.1	890.4 ± 28.32	0.907 ± 0.067
F8	0.20	0.30	0.1	440.5 ± 17.23	0.364 ± 0.174
F9	0.20	0.40	0.1	401.8 ± 13.13	0.318 ± 0.239
F10	0.20	0.50	0.1	318.2 ± 16.78	0.302 ± 0.074
F11	0.20	0.60	0.1	352.8 ± 21.97	0.313 ± 0.086
F12	0.20	0.80	0.1	584.6 ± 32.53	0.550 ± 0.099
F13	0.30	0.30	0.1	655.9 ± 30.36	0.605 ± 0.093
F14	0.30	0.40	0.1	637.6 ± 45.89	0.720 ± 0.064
F15	0.30	0.50	0.1	556.2 ± 15.52	0.811 ± 0.051
F16	0.40	0.30	0.1	960.4 ± 21.61	0.507 ± 0.097
F17	0.40	0.40	0.1	922.5 ± 69.23	0.818 ± 0.031
F18	0.40	0.50	0.1	874.7 ± 58.11	0.736 ± 0.071
F19	0.40	1.20	0.1	2333.7 ± 80.26	0.985 ± 0.104

inference may suggest that as sodium alginate concentration increases, the medium's viscosity rises, interfering with the degree of interaction between the polymer and the crosslinker and leading to the formation of different types of particles with significantly altered distribution patterns. The optimized batch F10 (0.2%w/v sodium alginate and 0.5%v/v chlorhexidine gluconate and 0.1%v/v tween) resulted smallest particle size and distribution. This batch was further used to prepare nanospray-dried porous nanoaggregates.

Characteristics of Spray-Dried Powder

Particle size and PDI

Particle size and PDI of the optimized batch post spray drying was found to be 184.5 ± 9.3 nm and 0.224 ± 0.1, respectively (Fig. 2). Lactose and leucine helped to increase the yield of the prepared nanoparticles. The size and PDI was observed to be reduced after spray drying. Lactose coating transformed the particles into hydrophilic, free-flowing and enhances the flavor of the final compositions [28]. Leucine's allowed it to lower the surface tension of the aqueous feedstock prior to drying. As a result, the size of the droplets created during atomization decreased, resulting in the creation of smaller particles with porous surface [29].

FTIR of Pure Drug and Spray-Dried Formulation

The IR spectrum of chlorhexidine gluconate is shown in (Fig. 3). The IR spectrum of the sample was compared with physical mixture and spray-dried powder. Table II shows the frequency of observed bands. The major band of the drug was found to be at 3345, 1965, 1439, 1416, 1063, 982, and 846 cm^{-1} could be representative peaks of N–H stretching (amine), C = C stretching (Arene), C-H bending (CH2), C-H bending (CH3), C-H in plane bend, O–H bend (Alcohol/phenol), and C-H bend (CH2), respectively. N–H stretching (amine), C = C stretching (Arene), C-H bending (CH2), C-H bending (CH3), C-H in plane bend, and C-H bend (CH2) peaks of the drug were present in the spray-dried powder at 3384, 1558, 1437, 1407, 1072, and 846 cm^{-1} except O–H bend (alcohol/phenol). It was the only peak that got disappeared from the drug peak. This could be due to the formation of hydrogen bond between two hydrophilic portion of the molecules. It portrays the presence of strong physical interaction between drug and polymer used [30].

Flow Properties of Spray-Dried Formulation

The assessment of the powdered flow property was done onthe basis of bulk density, tapped density, Carr's index, Hausner's ratio, and angle of repose. The results related to flow property is given in Table III. The empirical relation between the flow properties and the repose angle is established with the following

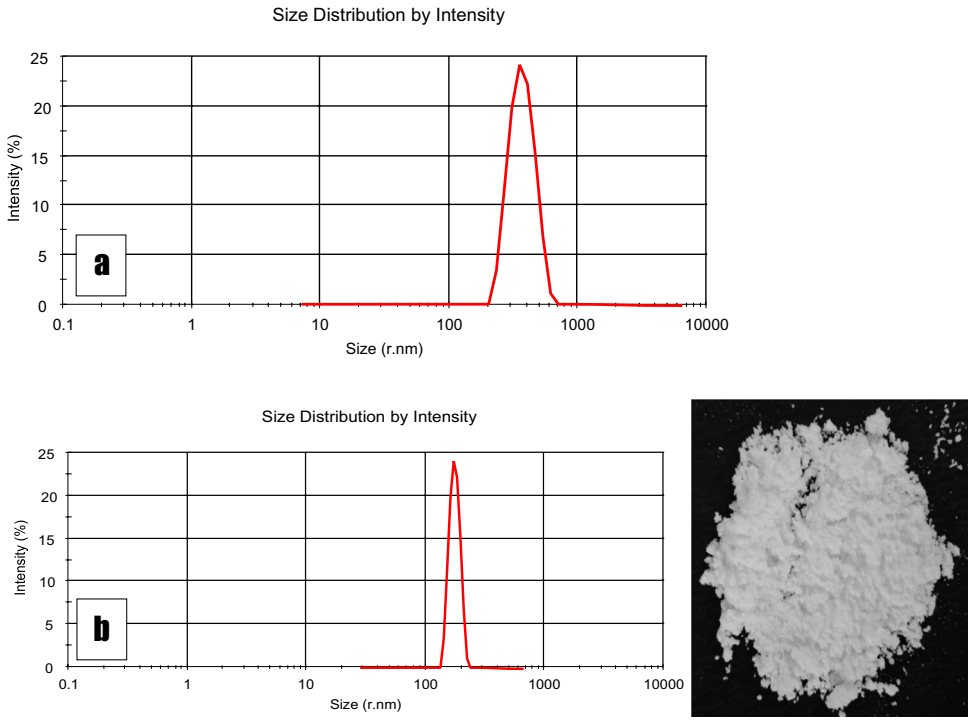

Fig. 2 Particle size and PDI of the nanoformulations. **a** Particle size distribution curve of nanoparticle and **b** particle size distribution curve of nanospray-dried powder

grading. The criteria for flowability are as follows. Flow property considered excellent if the angle of repose value is < 25°; for good flow property, the value should be between 25 and 30°; for passable, it should be between 30 and 40°; and for very poor, it should be > 40°. Hausner's ratio is also a good prediction of flow property. If this ratio is between 1.00 and 1.11, the flow property will be considered excellent. If this ratio is between 1.12 and 1.18, the flow property will be good. Ratio 1.19 to 1.25 portrays fair flow property, between 1.26 and 1.34 portrays passable flow, between 1.35 and 1.45 is poor flow, and however if it is between 1.46 and 1.59, it portrays very poor flow property. Carr's index values are another form of depiction of the flow property. Excellent flow means Carrs's index value ≤ 10%, good flow is considered if the Carr's index values are between 11 and 15%. Fair flow is depicted by Carr's index values between 16 and 20%, passable between 21 and 25%, poor between 26 and 31%, very poor between 32 and 37%, and very, very poor means value > 38%.

Based on these criteria, the angle of repose, which was observed to be 24–28°, can be considered having good flow property. The Hausner's ratio between 1.15 and 1.23 portrays good to fair flow property. However, Carr's index between 15 and 18% depicts fair flow property with very close bulk and tapped density, i.e., 0.64 and 0.68 g/cm^3, respectively. Closeness in these densities portrays dense nature of powder. Air gaps are not present, and hence, the powder is not fluffy. Fluffiness is inversely related to the flow property; hence, the data depicts good flowability of the powdered sample. From the results, it is seen that the spray-dried formulation is having good to excellent flow properties [31].

SEM Images of Optimized Formulation

Optimized formulation was visualized under SEM for surface morphology. SEM photographs revealed that spray-dried formulations were of spherical shape, porous aggregates (Fig. 4a). This porous structure is thought to provide enormous surface area for interaction with the biological media [32] and mucosal membrane owing to which enhanced mucoadhesiveness can be observed. Mucoadhesive behavior will lead to improvised localization of the particles at the desired site. Alginate matrix is usually crosslinked in the presence of ionic crosslinker in gel form and shrinks to smaller size slowly with time. However, once it is sprayed in the presence of lactose and leucine for drying in the air lead to rapid loss of water. That tends to form a porous structure as spray drying did not let to offer sufficient time for the polymer to go slow shrinking of the polymer network in the presence of environmental factors. This seems to be consistent with our XSEM images, where the particles are observed with the shell-like feature comprising enormous surface area as compared to the conventional alginate beads of spherical shape. This will also lead to the enhanced solubility of the drug at the mucosal site having aided with the desired potential against microbial infections.

XRD Analysis

This investigation is carried out to get idea about the presence of crystallinity in the tested powder. The physicochemical properties of a drug change by a transition from

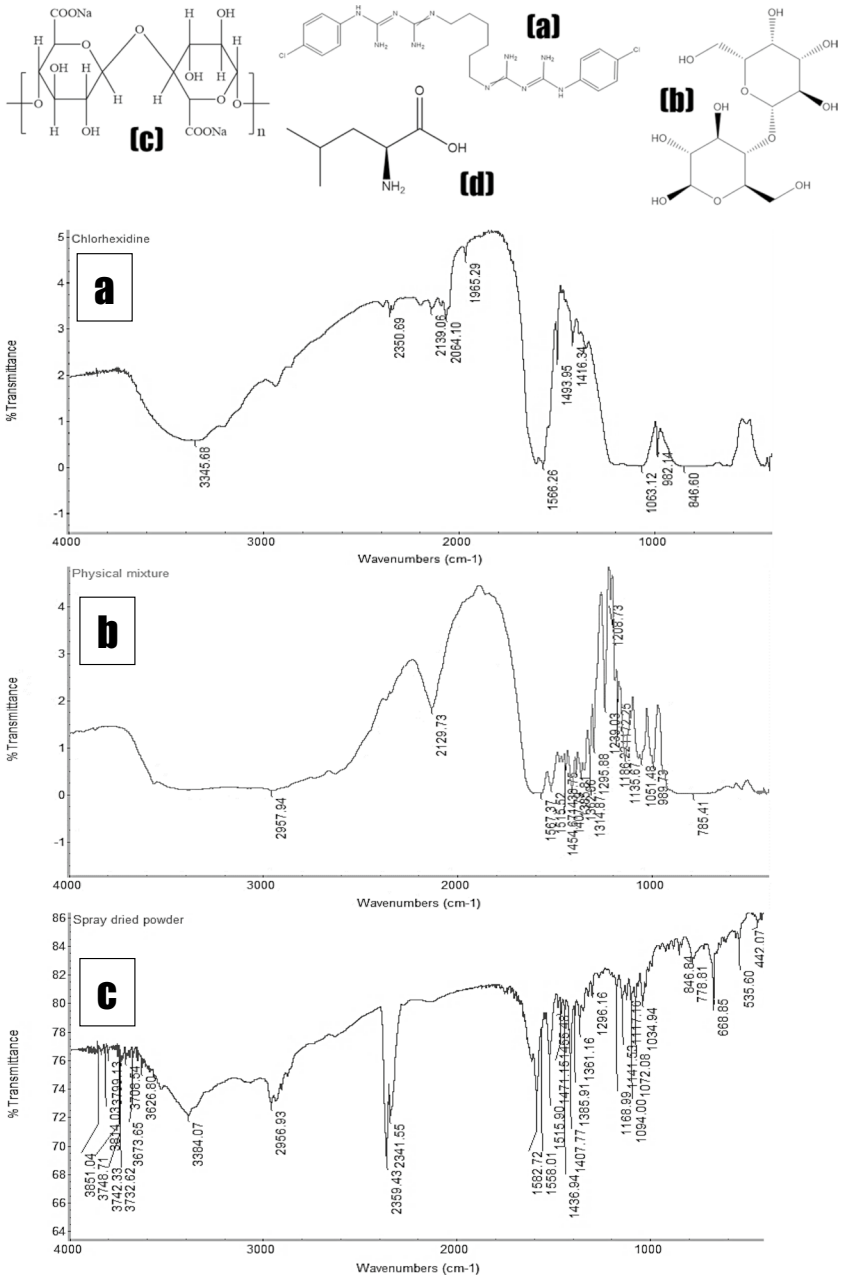

Fig. 3 FTIR spectra of the tested samples. **a** pure drug, **b** physical mixture and **c** spray-dried formulation. (a), (b), (c), and (d) depicts the molecular structure of chlorhexidine, lactose, sodium alginate and leucine, respectively

a crystalline state to amorphous state. Figure 4b and c are depicting the X-ray pattern curve of pure drug and its spray-dried nanoaggregates. The major peak characteristic peaks of drug at angle of 2θ are 20.14, 20.53, 22.95, 23.60, 24.90, 25.90, 26.95, 28.75, 31.65, 32.75, 36.20, 38.80, 41.05, 42.80, 44.15, 47.10, and 50.00. These peaks depict well characterized crystalline structure of the drug with very sharp peaks and high intensity. The major peaks of the spray-dried powder were present at 2θ = 3.10, 5.30, 11.70, 12.80, 13.00, 15.40, 16.60, 17.75, 18.90, 19.10, 19.40, 20.30, 20.90, 22.20, 23.60, 24.50, 24.90, 25.10, 25.90, 30.65, 31.05, 31.95, 32.75, 33.45, 35.65, 36.20, 37.20, 38.15, and 39.85. The spray-dried powder showed a greater number of peaks only 5 peaks in common with that of the pure chlorhexidine at 2θ value of 23.60, 24.90, 25.90, 32.75, and 36 (depicted in blue color). Other peaks are either sifted, miniaturized, or disappeared. Few new peaks were observed in the spectra of spray-dried powder that is expected to be due the presence of lactose [33] and leucine [34] at 2θ value of 11.70, 12.80, 16.60, 19.40, 20.30, 20.90, 24.50, 31.05, and 37.20 (depicted in green color). Sodium alginate is present in halo form that does not reveal any crystalline peak [35]. Some peaks could not be confirmed and considered unique. These peaks could not be identified either from chlorhexidine or from lactose and leucine. These could be the result deviations and formation of new form of crystals while spray drying [36].

Table II Characteristic FTIR Peaks of Drug and Spray-Dried Powder

Peak name	Group name	Chlorhexidine	Physical mixture	Spray-dried powder
N–H	Amine	3345	–	3384
O–H	Acid	–	2957	2956
C = C	Arene 1450–1600 medium 1660–2000 weak	1965	1566	1558
C-H bend	Methylene	1439	1438	1437
C-H bend	Methyle	1416	1407	1407
C-N stretch	1° or 2° amine	–	1314	–
C–O–C stretch	Ethers	–	1295	1296
		–	1239	–
		–	1186	–
C-O stretch	Alcohol/ether	–	1172	1168
		–	1135	1141
		–	–	1117
C-O stretch	Ester or acid Sp3	–	–	1094
C-H in plane bend		1063	1051	1072
O–H bend	Alcohols/phenols	982	989	Disappeared
C-H bend	Methylene CH2	846	–	846

Table III Flow Properties of Chlorhexidine Gluconate–Loaded Sodium Alginate Nanoparticles after Spray Drying

Flow properties	Bulk density	Tapped density	Carr's index	Hausner's ratio	Angle of repose
Results obtained	0.64 g/cm^3	0.68 g/cm^3	15–18%	1.15–1.23	24–28°

Entrapment Efficiency

Entrapment efficiency of the optimized batch "F10" was determined and repeated thrice. The physicochemical properties of sodium alginate played a key role in achieving high entrapment efficiency. The entrapment efficiency was calculated to be 87 ± 1.5%. Further coating with leucine and aided with lactose helped minimize leakage of the drug from spray-dried nanoparticles.

In Vitro Drug Release

In vitro drug release profile of the final formulation, marketed formulation, and plain drug is depicted in Fig. 5. Release profile of chlorhexidine gluconate showed initial fast release in 60 min. As much as 58% release could be observed in 1 h. However, marketed formulation showed very fast release (nearly 67%) in 60 min. This may be due to the higher solubilization effect in the case of marketed formulation. The developed formulation of chlorhexidine gluconate showed relatively slow-release rate (46%) as compared to plain drug and marketed formulation at the same time point. This may be due to the extra coating of leucine on alginate nanoparticle. The release pattern of spray-dried powder was found to be slow and uniform that gave nearly 72% drug release 360 min compared to pure drug and marketed formulation that gave 92 and 98% drug release, respectively at the same time point. The sustained effect of the polymeric nanoparticle was expected to contribute enhanced effect for longer duration against microbial infection if administered locally at the site of action [37].

In Vitro Drug Release Kinetics

To avoid significantly underestimating the drug release from nanoparticles, the release tests were carried out in sink circumstances. Therefore, the drug solubilization in each release profile as a function of time is known as kinetics. The *in vitro* drug release profiles of the spray-dried formulation were plotted against pure chlorhexidine gluconate and its marketed formulation in Fig. 5. The same release profiles were subjected to various release kinetics models, and their respective curves are presented in Fig. 5. The developed spray-dried product of chlorhexidine gluconate is seemed to follow Higuchi model owing to its higher R^2 value, i.e., 0.959, when compared with first order kinetic, zero order, and Peppas model having R^2 values 0.943, 0.885, 0.835, respectively. According to the Higuchi model, the initial drug concentration was significantly higher owing to which a fast release was observed initially. The drug gradually expulsed out of the matrix when the surrounding fluid enters as per the Fick's first law of diffusion from a polymer matrix. It seems that the developed nanoparticles are following dissolution-controlled release kinetics where the rate at

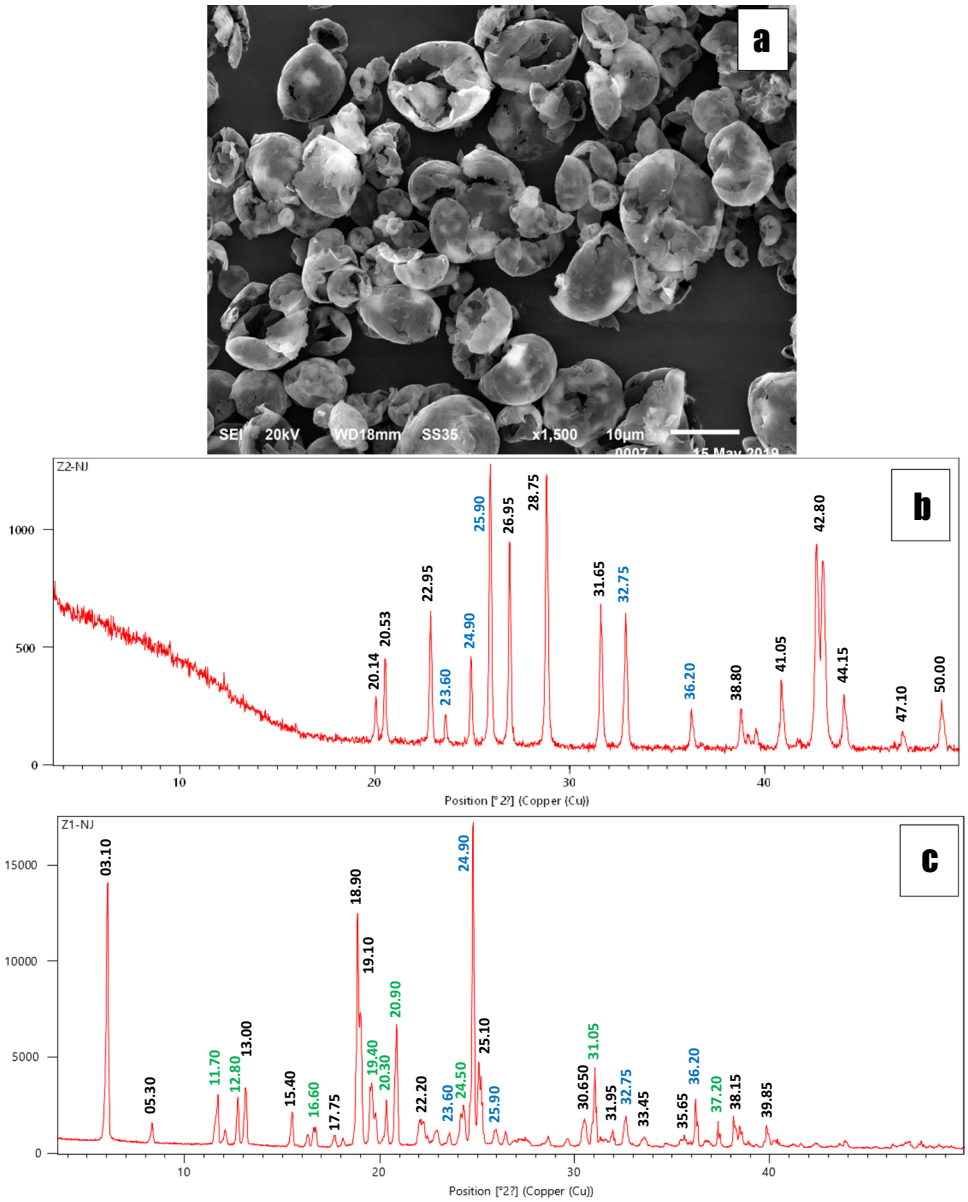

Fig. 4 SEM image and X-ray diffraction curves of chlorhexidine gluconate–loaded spray-dried formulation. **a** SEM image of the developed spray-dried particles depicting porous nanoaggregates of the drug; **b** and X-ray diffraction curve of pure chlorhexidine gluconate depicting well characterized crystalline structure; and **c** X-ray diffraction curves of chlorhexidine gluconate–loaded spray-dried formulation

which the drug dissolved from the particle matrix was more than the diffusional processes. However, it may not be possible when the drug dissolves very slowly. Slow dissolution might be expected for drugs having low solubility in the matrix [38].

Ex Vivo Permeation Profile of the Developed Formulation

Figure 6 shows the *ex vivo* comparative permeation profile of pure chlorhexidine gluconate, its spray-dried nanoparticle, and marketed formulation through goat intestine. Plain drug, owing to its direct exposure at permeation site, portrayed highest degree of permeation (nearly 91.26%) at 6th h of the study followed by marketed formulation (nearly 80.56%) and optimized formulation (66.03%). No drug permeation was observed in the case of pure drug after 6th h and marketed formulation showed almost 96% drug release after 480 min or 8th h. But the developed formulation showed controlled drug permeation (87.29% in 720 min) for 12 h and still had capacity to provide drug consistently. It is the known fact that, permeation profile depends on the drug release from the formulation [39]. A controlled release rate controls the rate of drug permeation and hence ensures consistent drug availability at the desired site of action. One more benefit of controlled permeation is that, it does not let the dissolution media saturated owing to its slow and consistent supply of the drug. However, sample with fast permeation rate may sometime cause saturation of the administration site

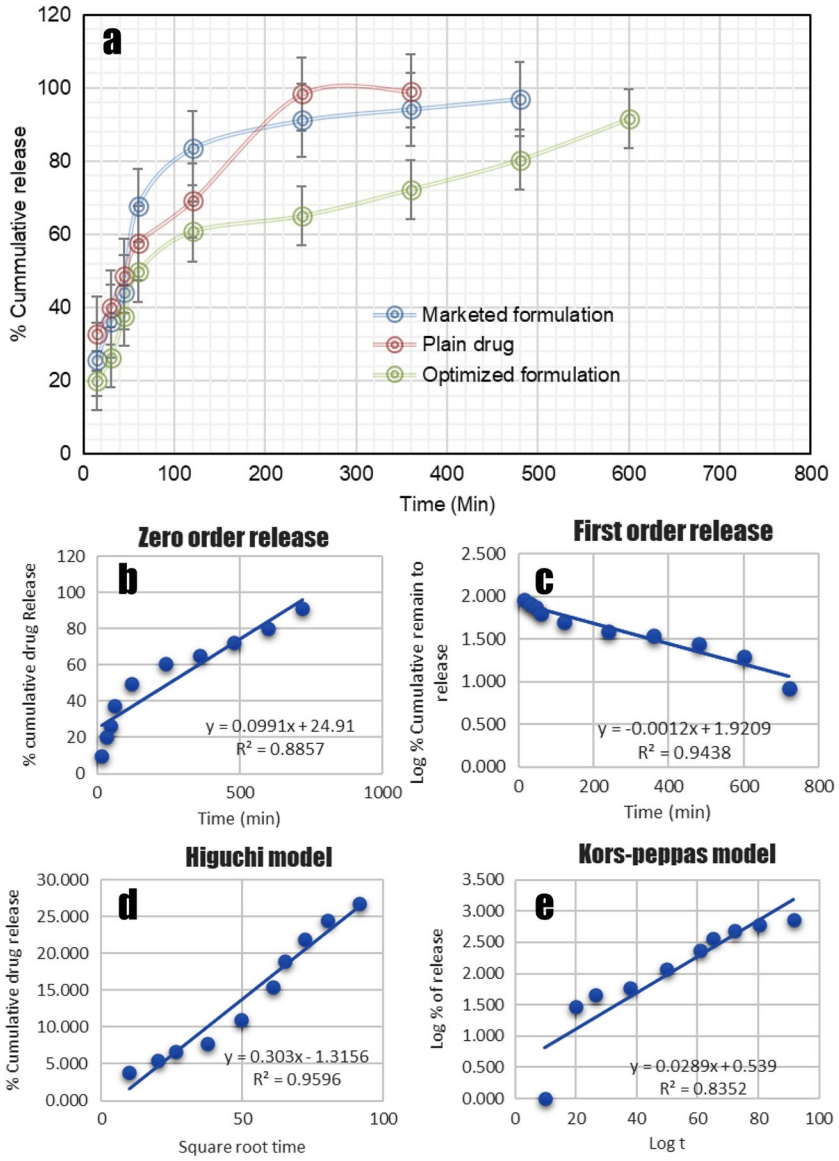

Fig. 5 Graphical depiction of *in vitro* drug release profile and release kinetic of optimized spray-dried formulation. **a** Cumulative drug release profile, **b** zero order release kinetics model, **c** first order release kinetics model, **d** Higuchi release kinetics model, **e** Kors–Peppas kinetics model

owing to which further drug release and permeation may be retarded.

Mucoadhesion Strength

Mucoadhesiveness strength study in the direct reflection of time of drug stay at the desired localized site. It ensures the retention of the drug carrier at the absorption site. The mucoadhesiveness of the optimized spray-dried formulation shows sufficient mucoadhesive detachment force (100 g/cm^2) to ensure easy retention at the buccal mucosa (Fig. 6). The mucoadhesive property was observed by using a texture analyzer (CT-3, Brookfield) [40].

Antimicrobial Potential of the Developed Spray-Dried Powder

Zone of growth inhibition (ZGI) was determined from an antimicrobial well diffusion assay method. Equal strength of pure chlorhexidine gluconate, its nanoparticle, and marketed formulation were subjected to the antimicrobial investigation. After comparison of the ZGI in the tested microbe, ZGI in the case of pure chlorhexidine gluconate was found to be 2.10 ± 0.19 cm; however, its value in the case of marketed and developed formulation was observed to be 2.87 ± 0.14 cm and 2.63 ± 0.12 cm. Figure 7 and Table IV show zone of growth inhibition of tested microbe treated with pure chlorhexidine gluconate, its nanoparticle, and marketed formulation, which

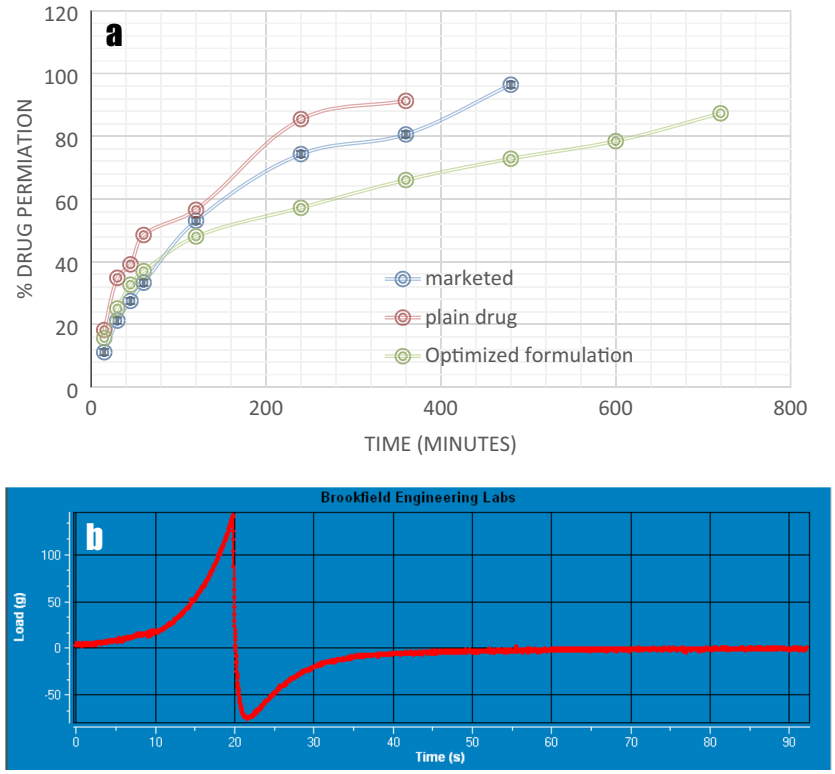

Fig. 6 Pictorial depiction of an *ex vivo* drug permeation and texture profile analyzing mucoadhesion of spray-dried formulation. **a** Drug permeation profile and **b** texture profile

indicate that optimized spray-dried powder has significantly more anti-microbial activity than pure drug and it is quite comparable with marketed formulation [41].

In Vivo Study by X-Ray Analysis

The mucoadhesive behaviors of the developed formulation mean to improvise the drug retention at the desired mucosal site. Retention efficacy of optimized formulation in rat was determined using radiographic imaging technique. Figure 7 illustrates X-ray imaging of animals administered with the placebo and spray-dried formulation at 3rd h, 5th h, and 8th h of the study period. The spray dried powder containing barium sulfate as contrast agent was used to determine the retention time of the prepared formulation. Results show that the prepared mucoadhesive formulation was retained in the throat for prolonged time (8 h). The X-ray analysis further ensures that the prepared formulation retained at the throat region [27]. Extended retention at the throat region of the mouth might ensure improvised efficacy against potential throat infections including those observed frequently during rainy and winter seasons.

The study was an attempt to develop chlorhexidine-loaded mucoadhesive gargle for the treatment of throat infection. Due to its mucoadhesive property, its gargle is expected to remain in the oral cavity and release its drug content for a long period of time, thus providing diffusion-controlled drug release. The nanoparticles were formed by the ion-gelation method. Lactose and leucine have been used to modify the yield of the nanoparticles. Coating of lactose and leucine make the particles hydrophilic and modify the taste [42]. Leucine's surfactant qualities allow it to lower the surface tension of the aqueous feedstock prior to drying. As a result, the size of the droplets created during atomization decreases, resulting in the creation of smaller particles. The droplet then develops a crystalline shell made of leucine, which offers mechanical resistance to the confined water vapor's escape. The leucine shell develops a corrugated surface as a result of various degrees of plastic expansion caused by vapor pressure. Leucine produces a semipermeable, incoherent shell when the concentration of leucine at the droplet's surface is insufficient to create a coherent shell, which allows water vapor to pass through and lead to ruptured particles [43].

Conclusion

Chlorhexidine-loaded nanoparticles for throat infection were prepared by optimizing the formulation by varying the quantities of sodium alginate and chlorhexidine. The best formulation had a particle size of 318.2 ± 9.3 nm with good entrapment efficiency and flow properties. The formulation showed sustained release over a duration of 10 h while about 87% drug permeated within 12 h. It was also observed to have good mucoadhesive strength as obtained

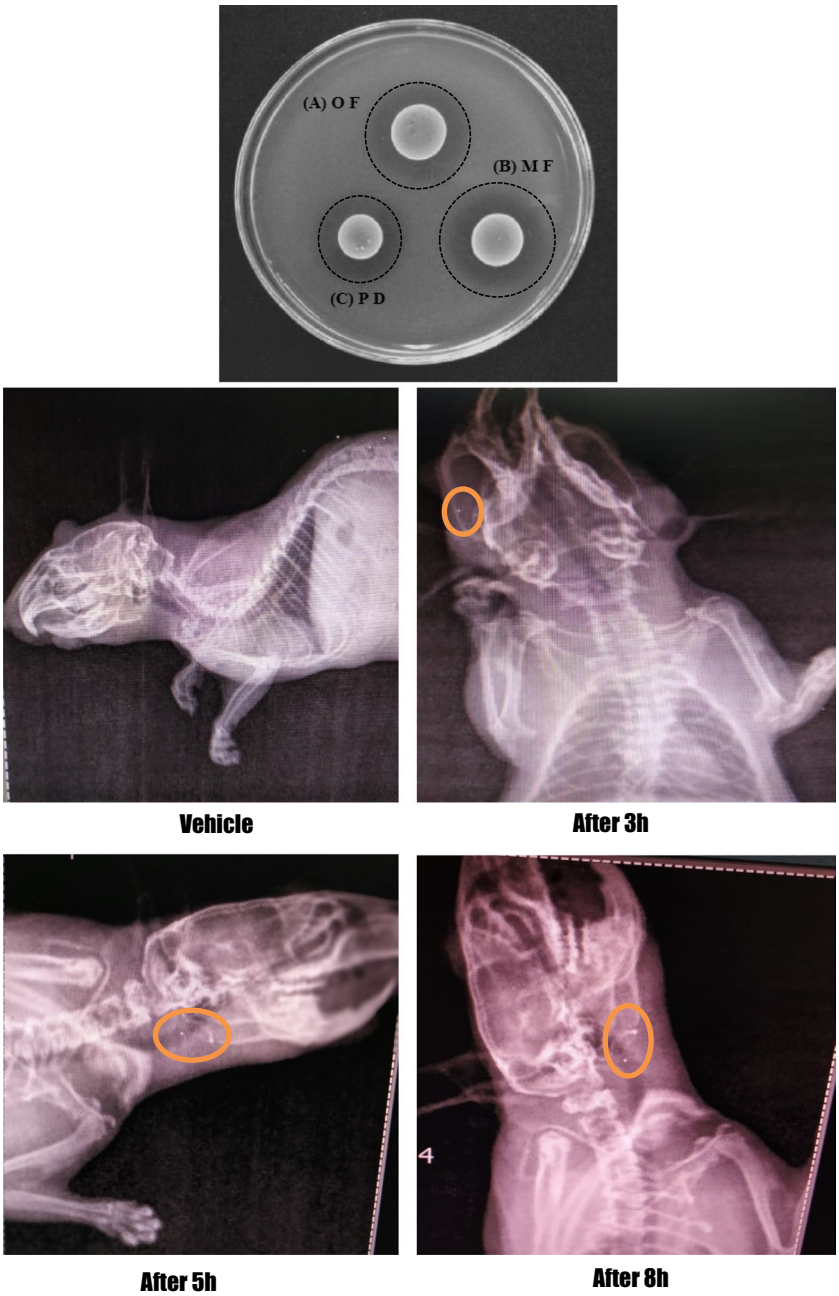

Fig. 7 Comparative zone of growth inhibition of *S. aureus* treated with pure chlorhexidine gluconate, its nanoparticle, and marketed formulation along with pictorial depiction of imaging of barium sulfate–containing mucoadhesive gargle in the throat after oral administration of vehicle, and spray-dried nanoparticle. **a** Optimized formulation; **b** marketed formulation; **c**, plain drug. X-ray images of mice treated with vehicle and the developed barium sulfate–containing mucoadhesive gargle at 3rd, 5th, and 8th h of the investigation

Table IV Zone of Growth Inhibition of Tested Microbe Treated with Pure Chlorhexidine Gluconate, Its Nanoparticle, and Marketed Formulation

Formulations	Zone of inhibitions in cm (*S. aureus*), $n=3$
Chlorhexidine gluconate	2.10 ± 0.19 cm
Optimized formulation	2.63 ± 0.12 cm
Marketed formulation	2.87 ± 0.14 cm

from texture analyzer. As compared to marketed formulation or pure drug, the formulation was observed to exhibit better zone of growth inhibition against *S. aureus*. *In vivo* retention of bio-adhesive nanoparticles in throat of mice was observed by X-ray analysis of real time moment of barium sulfate–loaded nanoparticles. Thus, these nanoparticles portrayed good mucoadhesion *in vivo* and had comparative antimicrobial efficiency with marketed formulation or pure drug. Therefore, the formulation can be considered as a potential candidate for the treatment of throat infection, for which the powder form can be reconstituted in water before usage thus leading to improved palatability.

Acknowledgements The authors acknowledge the Researchers Supporting Project number (RSPD2024R708), King Saud University, Riyadh, Saudi Arabia, for funding this research work. The authors also acknowledge the financial support of the Department of Biotechnology (DBT), Govt. India.

Author Contributions Vineet Kumar Rai: data collection, experimental work, compilation, and manuscript writing. Amresh Kumar: data collection and experimental work. Deepak Pradhan: proof reading, software and language editing. Jitu Halder: data analysis, language editing and critical analysis. Tushar Kanti Rajwar: compilation, manuscript writing. Manoj Kumar Sarangi: data collection, experimentation and statistics. Priyanka Dash: animal experimentation and proof reading. Chandan Dash: software analysis, data collection, and proof reading. Salim Manoharadas: data analysis, language editing, and funding support. Biswakanth Kar: animal experiment and data interpretation. Goutam Ghosh: conceptualization of the topics and critical analysis. Goutam Rath: conceptualization of the topic and design of the table of content, supervision, data analysis, and paper writing, editing, and proof reading.

Funding The research was funded by the DBT Builder project with order no. (BT/INF/22/SP45078/2022).

Declarations

Human and Animal Rights The animal protocol used in this study was approved by the Institutional Animal Ethical Committee (IAEC) bearing Regd. No IAEC/SPS/SOA/122/2022.

Conflict of Interest All the authors declare no conflict of interest.

References

1. Macedo AS, Castro PM, Roque L, Thomé NG, Reis CP, Pintado ME, et al. Novel and revisited approaches in nanoparticle systems for buccal drug delivery. J Control Release. 2020;320:125–41.
2. Montenegro-Nicolini M, Morales JO. Overview and future potential of buccal mucoadhesive films as drug delivery systems for biologics. AAPS PharmSciTech. 2017;18:3–14.
3. Gilhotra RM, Ikram M, Srivastava S, Gilhotra N. A clinical perspective on mucoadhesive buccal drug delivery systems. J Biomed Res. 2014;28(2):81.
4. Pathan SA, Iqbal Z, Sahani JK, Talegaonkar S, Khar RK, Ahmad F, et al. Buccoadhesive drug delivery systems-extensive review on recent patents. Recent Patents Drug Deliv Formul. 2008;2(2):177–88.
5. Russo E, Selmin F, Baldassari S, Gennari C, Caviglioli G, Cilurzo F, et al. A focus on mucoadhesive polymers and their application in buccal dosage forms. J Drug Deliv Sci Technol. 2016;32:113–25.
6. Morales JO, Brayden DJ. Buccal delivery of small molecules and biologics: of mucoadhesive polymers, films, and nanoparticles. Int J Pharm. 2017;36:22–8.
7. Shridhar GS, Manohar SD, Bhanudas SR. Mucoadhesive buccal drug delivery: an overview. J Adv Pharm Technol Res. 2013;3(4):319–32.
8. Wang T, Fleming E, Luo Y. An overview of the biochemistry, synthesis, modification, and evaluation of mucoadhesive polymeric nanoparticles for oral delivery of bioactive compounds. Adv Compos Hybrid Mater. 2023;6(1):6.
9. Pal D, Nayak AK. Novel tamarind seed polysaccharide-alginate mucoadhesive microspheres for oral gliclazide delivery: in vitro–in vivo evaluation. Drug Deliv. 2012;19(3):123–31.
10. Md S, Ahuja A, Khar RK, Baboota S, Chuttani K, Mishra A, et al. Gastroretentive drug delivery system of acyclovir-loaded alginate mucoadhesive microspheres: formulation and evaluation. Drug Deliv. 2011;18(4):255–64.
11. Patil SB, Sawant KK. Development, optimization and in vitro evaluation of alginate mucoadhesive microspheres of carvedilol for nasal delivery. J Microencapsul. 2009;26(5):432–43.
12. Nayak AK, Pal D. Formulation optimization and evaluation of jackfruit seed starch–alginate mucoadhesive beads of metformin HCl. Int J Biol Macromol. 2013;59:264–72.
13. Garner S, Barbour ME. Nanoparticles for controlled delivery and sustained release of chlorhexidine in the oral environment. Oral Dis. 2015;21(5):641–4.
14. Tokajuk G, Niemirowicz K, Deptuła P, Piktel E, Cieśluk M, Wilczewska AZ, et al. Use of magnetic nanoparticles as a drug delivery system to improve chlorhexidine antimicrobial activity. Int J Nanomed. 2017;12:7833.
15. Seneviratne CJ, Leung KC-F, Wong C-H, Lee S-F, Li X, Leung PC, et al. Nanoparticle-encapsulated chlorhexidine against oral bacterial biofilms. Plos One. 2014;9(8):e103234.
16. Saha I, Palak A, Rai VK. Relevance of NLC-gel and microneedling-assisted tacrolimus ointment against severe psoriasiform: in vitro dermal retention kinetics, in vivo activity and drug distribution. J Drug Deliv Sci Technol. 2022;71: 103272.
17. Zhan YR, Chen P, He X, Hei MW, Zhang J, Yu XQ. Sodium alginate-doping cationic nanoparticle as dual gene delivery system for genetically bimodal therapy. Biomacromol. 2022;23(12):5312–21.
18. Cui Y, Zhang X, Wang W, Huang Z, Zhao Z, Wang G, et al. Moisture-resistant co-spray-dried netilmicin with l-leucine as dry powder inhalation for the treatment of respiratory infections. Pharmaceutics. 2018;10(4):252.
19. Zimmermann CM, Baldassi D, Chan K, Adams NBP, Neumann A, Porras-Gonzalez DL, et al. Spray drying siRNA-lipid nanoparticles for dry powder pulmonary delivery. J Control Release. 2022;351:137–50.
20. Zhou Q, Armstrong B, Larson I, Stewart PJ, Morton DA. Improving powder flow properties of a cohesive lactose monohydrate powder by intensive mechanical dry coating. J Pharm Sci. 2010;99(2):969–81.
21. Iida K, Hayakawa Y, Okamoto H, Danjo K, Leuenberger H. Evaluation of flow properties of dry powder inhalation of salbutamol sulfate with lactose carrier. Chem Pharm Bull. 2001;49(10):1326–30.
22. Shrimal P, Jadeja G, Patel S. Microfluidics nanoprecipitation of telmisartan nanoparticles: effect of process and formulation parameters. Chem Pap. 2021;75(1):205–14.
23. Surjit Singh CK, Lim HP, Tey BT, Chan ES. Spray-dried alginate-coated Pickering emulsion stabilized by chitosan for improved oxidative stability and in vitro release profile. Carbohyd Polym. 2021;251: 117110.
24. Rai VK, Yadav NP, Sinha P, Mishra N, Luqman S, Dwivedi H, et al. Development of cellulosic polymer based gel of novel ternary mixture of miconazole nitrate for buccal delivery. Carbohyd Polym. 2014;103:126–33.
25. Sharma A, Upadhyay DK, Sarma GS, Kaur N, Gupta GD, Narang RK, et al. Squalene integrated NLC based gel of tamoxifen citrate for efficient treatment of psoriasis: a preclinical investigation. J Drug Deliv Sci Technol. 2020;56: 101568.
26. Pattnaik S, Subramanyam VR, Bapaji M, Kole CR. Antibacterial and antifungal activity of aromatic constituents of essential oils. Microbios. 1997;89(358):39–46.
27. Kang RK, Mishr N, Rai VK. Guar gum micro-particles for targeted co-delivery of doxorubicin and metformin HCL for improved specificity and efficacy against colon cancer: in vitro and in vivo studies. AAPS PharmSciTech. 2020;21(2):48.

28. Sateesha S, Rajamma A, Shekar H, Divakar G. Formulation development and rheological studies of palatable cefetamet pivoxil hydrochloride dry powder suspension. Daru. 2011;19(2):118–25.
29. Li N, Li X, Yang P, Liu H, Kong L, Yu X. Microencapsulation of Fe2+ in spray-dried lactose for improved bioavailability. Bioinorg Chem Appl. 2021;2021:5840852.
30. Wairkar S, Gaud R. Development and Characterization of Microstructured, Spray-Dried Co-Amorphous Mixture of Antidiabetic Agents Stabilized by Silicate. AAPS PharmSciTech. 2019;20(3):141.
31. Rathod P, Mori D, Parmar R, Soniwala M, Chavda J. Co-processing of cefuroxime axetil by spray drying technique for improving compressibility and flow property. Drug Dev Ind Pharm. 2019;45(5):767–74.
32. Show K-Y, Yan Y-G, Lee D-J. Algal biomass harvesting and drying. Biofuels from Algae: Elsevier; 2019. p. 135–66.
33. Kou X, Chan LW, Sun CC, Heng PWS. Preparation of slab-shaped lactose carrier particles for dry powder inhalers by air jet milling. Asian J Pharm Sci. 2017;12(1):59–65.
34. Lamy B, Serrano D, O'Connell P, Couet W, Marchand S, Healy A, et al. Use of leucine to improve aerodynamic properties of ciprofloxacin-loaded maltose microparticles for inhalation. Eur J Pharm Res. 2019;1:02–11.
35. Aburahma MH, Mahmoud AA. Biodegradable ocular inserts for sustained delivery of brimonidine tartarate: preparation and in vitro/in vivo evaluation. AAPS PharmSciTech. 2011;12(4):1335–47.
36. Wijiani N, Isadiartuti D, Rijal MAS, Yusuf H. Characterization and dissolution study of micellar curcumin-spray dried powder for oral delivery. Int J Nanomed. 2020;15:1787–96.
37. Sipos B, Csóka I, Ambrus R, Schelz Z, Zupkó I, Balogh GT, et al. Spray-dried indomethacin-loaded polymeric micelles for the improvement of intestinal drug release and permeability. Eur J Pharm Sci. 2022;174: 106200.
38. Dash S, Murthy PN, Nath L, Chowdhury P. Kinetic modeling on drug release from controlled drug delivery systems. Acta Pol Pharm. 2010;67(3):217–23.
39. Sinha P, Srivastava N, Rai VK, Mishra R, Ajayakumar PV, Yadav NP. A novel approach for dermal controlled release of salicylic acid for improved anti-inflammatory action: combination of hydrophilic-lipophilic balance and response surface methodology. J Drug Deliv Sci Technol. 2019;52:870–84.
40. Rai VK, Roy A, Sharma A, Rath G, Kar B, Ghosh G, et al. Development and pharmaceutical evaluation of azelaic acid and vitamin E oil-based nanoemulgel of tacrolimus for topical application in plaque psoriasis. J Pharm Innov. 2023;18:1616–25.
41. Charannya S, Duraivel D, Padminee K, Poorni S, Nishanthine C, Srinivasan MR. Comparative evaluation of antimicrobial efficacy of silver nanoparticles and 2% chlorhexidine gluconate when used alone and in combination assessed using agar diffusion method: an in vitro study. Contemp Clin Dentist. 2018;9(2):S204–9.
42. Thiyagarajan D, Huck B, Nothdurft B, Koch M, Rudolph D, Rutschmann M, et al. Spray-dried lactose-leucine microparticles for pulmonary delivery of antimycobacterial nanopharmaceuticals. Drug Deliv Transl Res. 2021;11(4):1766–78.
43. Alhajj N, O'Reilly NJ, Cathcart HJ. Leucine as an excipient in spray dried powder for inhalation. Drug Discov Today. 2021;26(10):2384–96.